Phytochemistry 71 (2010) 1673–1683

Contents lists available at ScienceDirect

Phytochemistry

journal homepage: www.elsevier.com/locate/phytochem

Arabidopsis peroxidase-catalyzed copolymerization of coniferyl and sinapyl alcohols: Kinetics of an endwise process

Nathalie Demont-Caulet [a,b], Catherine Lapierre [a], Lise Jouanin [a], Stéphanie Baumberger [a], Valérie Méchin [a,*]

[a] Institut Jean-Pierre Bourgin, UMR 1318 INRA/AgroParisTech, Pôle Systèmes Cellulaires, Morphogénèse et Signalisation, 78850 Thiverval-Grignon, Cedex, France
[b] UFR des Sciences du Vivant, Université Diderot-Paris 7, 75205 Paris, Cedex 13, France

ARTICLE INFO

Article history:
Received 22 April 2010
Received in revised form 11 June 2010
Available online 6 July 2010

Keywords:
Coniferyl and sinapyl alcohols
Endwise
Bulk
Oligolignols structure
Lignin synthesis
Plant peroxidase

ABSTRACT

In order to determine the mechanism of the earlier copolymerization steps of two main lignin precursors, sinapyl (S) alcohol and coniferyl (G) alcohol, microscale *in vitro* oxidations were carried out with a PRX34 *Arabidopsis thaliana* peroxidase in the presence of H_2O_2. This plant peroxidase was found to have an *in vitro* polymerization activity similar to the commonly used horseradish peroxidase. The selected polymerization conditions lead to a bulk polymerization mechanism when G alcohol was the only phenolic substrate available. In the same conditions, the presence of S alcohol at a 50/50 S/G molar ratio turned this bulk mechanism into an endwise one. A kinetics monitoring (size-exclusion chromatography and liquid chromatography–mass spectrometry) of the different species formed during the first 24 h oxidation of the S/G mixture allowed sequencing the bondings responsible for oligomerization. Whereas G homodimers and GS heterodimers exhibit low reactivity, the SS pinoresinol structure act as a nucleating site of the polymerization through an endwise process. This study is particularly relevant to understand the impact of S units on lignin structure in plants and to identify the key step at which this structure is programmed.

1. Introduction

Lignin is a natural macromolecule resulting from the polymerization of three main monomers: *p*-coumaryl alcohol, coniferyl alcohol and sinapyl alcohol. *In vitro* preparation of synthetic lignins in the presence of oxidative systems such as peroxidase/H_2O_2 supports the idea that this polymerization mainly occurs via radical couplings. Such a polymerization process implies that phenolic groups of both the monolignol and the growing polymer are oxidized into radicals, either directly by the catalyst or by the radical transfer from another monolignol radical. The structure of the final polymer is therefore highly dependent on the oxidative system, the nature and proportion of monolignols and also on the physicochemical constraints. These parameters confer a high degree of plasticity to native and synthetic lignins. Understanding the chemical mechanisms of monolignols polymerization is thus of primary importance for both controlling the structure of synthetic lignins and the elucidation of lignification in plants.

Class III plant peroxidases are secreted plant enzymes that catalyze the oxidation of a wide variety of phenolic substrates, including monolignols. However, peroxidase affinity for the three different monolignols is different. While coniferyl alcohol is readily oxidized by most peroxidases, sinapyl alcohol often appears to be a poor substrate. Takahama and Oniki (1994) suggested that sinapyl alcohol oxidation *in planta* should be mediated by other phenolic radicals. This hypothesis has been strengthened by *in vitro* copolymerization experiments of sinapyl alcohol and coniferyl alcohol and of their glucosides (Tobimatsu et al., 2008a,b, 2010). However, some studies (Quiroga et al., 2000; Aoyama et al., 2002; Gabaldon et al., 2005; Marjamaa et al., 2006) have highlighted that some class III peroxidases display a highest affinity for sinapyl alcohol. Such peroxidases, called syringyl peroxidases, seem to be rather widespread in the plant kingdom (Barcelo et al., 2007). Whether both radical mediation and direct oxidation by peroxidases can account for the incorporation of syringyl units in lignins, the detailed mechanism of this incorporation has not yet been reported so far. Similarly, there are few reports in which the whole process of dehydrogenative polymerization of monolignols is monitored.

The objective of this study was to determine the impact of sinapyl alcohol on the polymerization mode of coniferyl alcohol and to elucidate the bonding sequences leading to the incorporation of sinapyl alcohol in the first steps of the oligomerization.

Using class III peroxidase purified from *Arabidopsis thaliana*, we have investigated the oxidation of either a mixture of sinapyl and coniferyl alcohol or sinapyl and coniferyl alcohols alone to determine the polymerization mode recruited in each condition. Kinetics of the monomer conversion and of the subsequent formation of di-, tri- and tetramers was carried out. We show that, in our *in vitro* oxidation conditions, the presence of S monomers converted the polymerization of G monomers from a bulk to an endwise mechanism. This result allowed us to confirm the role of coniferyl alcohol

* Corresponding author. Tel.: +33 1 30 81 54 62; fax: +33 1 30 81 53 73.
E-mail address: valerie.mechin@grignon.inra.fr (V. Méchin).

0031-9422/$ - see front matter © 2010 Elsevier Ltd. All rights reserved.
doi:10.1016/j.phytochem.2010.06.011

as radical mediator for sinapyl alcohol oxidation and identify key molecular structures associated with the incorporation of sinapyl alcohol. This study brings new information on the compared reactivity of S and S/G lignin model compounds.

2. Results and discussion

Oxidative coupling was carried out in three different substrate conditions: (i) coniferyl (G) alcohol alone, (ii) sinapyl (S) alcohol alone or (iii) a 50/50 mixture of both G and S alcohols, to trace the appearance and accumulation of oligomers synthesized without peroxidase or in the presence of either horseradish peroxidase (HRP) or PRX34 *A. thaliana* peroxidase (PRX34).

In order to over produce the protein PRX34 (gene At3g49120), we used two different Arabidopsis mutant lines derived from the Wassilewsija and Columbia ecotypes: (i) Atprx34 (FSTS51769) selected in the Salk collection. Atprx34 is a deregulated line with higher expression of the corresponding targeted gene at the stem level compared to the wild type. (ii) In order to visualize and over express PRX34, its cDNA under the control of the CaMV 35S promoter was cloned in the GFP Gateway vector pGWB5 and introduced in the Columbia ecotype.

The Atprx34 line over produced PRX34 three times whereas the fusion Perx34-GFP allowed an over production of fifteen times. The purified proteins have the same enzymatic activity and thus we decided to use protein purified from the transformed Columbia because of the higher purification yield.

Stems (5–6 week-old) of these two lines were harvested and used for peroxidase purification. Peroxidases were purified among a set of N-glycosylated proteins selected on a Concanavalin-A Sepharose column (Minic et al., 2007). The fraction containing the glycosylated proteins was further purified by carboxymethyl-Sepharose column. The activity peak was collected in each sample and loaded on an acrylamide gel further stained with silver nitrate or revealed with an antisera raised against bean peroxidase (Fig. 1). Maldi-TOF MS was used to identify the purified PRX34 through peptide mass fingerprinting after trypsin digestion of the bands. The obtained peptide masses led to the identification of PRX34 using the MSDB database Accession No. T46118, with at least thirteen matching peptides, covering 42% of the protein and with a mass accuracy inferior to 50 ppm. The protein has a calculated molecular mass of 38.8 kDa. This purified protein was used to perform subsequent oxidative coupling of G and S alcohols.

2.1. Monomers consumption during peroxidase-catalyzed homopolymerization

If no peroxidase is added in the reaction medium (data not shown), S alcohol begins to be consumed to produce dimers after 1 h, alone or in mixture with G alcohol. We never detected in these conditions any higher oligomers than polymerization degree (PD) 2. Even in combination with S alcohol, G alcohol is never used to form dimers or other products.

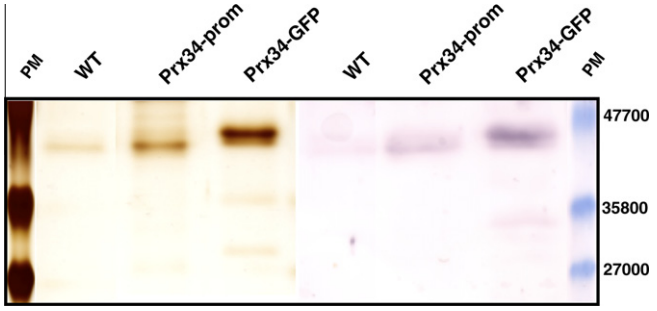

Fig. 1. SDS–PAGE and Western blot analysis of purified peroxidase using polyclonal antibodies raised against peroxidases. Pooled active fractions from purification stage were subjected to SDS–PAGE on 10% gels visualized by silver staining (left part) or by Western blot analysis (right part). WT: wild type line, PRX34-prom: over-expressed line, PRX34-GFP: fusionned protein PRX34 with GFP.

When adding peroxidase to the initial reaction medium, we obtained similar results while using either HRP or PRX34 peroxidase and thus decided to focus the paper on PRX34-catalyzed polymerization. If the only substrate is S alcohol, we observed as in the absence of peroxidase the appearance of dimers and the total consumption of S alcohol within 4 h (Fig. 2a). G alcohol alone is dimerized after 5 min (Fig. 3a) and is totally converted at 20 min (Fig. 2a). Trimers begin to appear at 10 min and tetramers at 30 min (Fig. 3a). Monomer conversion rate is thus far higher for G than for S alcohol (9-fold lower conversion time), which is in contradiction with the respective redox potential of these species (Tobimatsu et al., 2008c). This lower reactivity of S alcohol towards peroxidase oxidation is thus commonly explained by the low accessibility of S monomers to the peroxidase active site due to steric hindrance and hydrophobic effects of the two OCH_3 groups on the aromatic ring (Nielsen et al., 2001; Tobimatsu et al., 2008a).

2.2. Monomers consumption during peroxidase-catalyzed copolymerization

In the copolymerization conditions, all the monomers are converted within the first 30 min (Fig. 2b). S monomers are completely converted after 5 min (Fig. 2b). This result dramatically contrasts with the four hours required for the total conversion of S in homopolymerization conditions (Fig. 2a). Whereas the presence of G accelerates the conversion of S monomers, the presence of S slows down the conversion of G (10 additional minutes required for total conversion; Fig. 2a and b). This result was repeatedly observed using HRP peroxidase and is in agreement with the role of radical mediator assigned to G in various studies (Takahama et al., 1996; Aoyama et al., 2002; Fournand et al., 2003; Sasaki et al., 2004; Tobimatsu et al., 2008a) that confirm the earlier observation that G monomers take part in S monomers conversion (Freudenberg and Hubner, 1952). Once oxidized by peroxidase, G would transfer its radical to S consistently with the lower S redox potential. As proposed by Tobimatsu et al. (2008b), G monomers could also act as a promoter in the stoichiometric quenching of S-type quinone methide (QM) in the course of copolymerization by displacing the equilibrium and thus accelerate the conversion of stable S-type QM intermediates.

In order to elucidate the mechanisms by which S monomers are incorporated into the final polymer, we focused on the structure of the dimers and further higher oligomers formed. The structure of compound with a PD comprised from 2 to 4 were thus assigned according to their mass and photodiode array (PDA) spectra as reported by Morreel et al. (2004). As for the global monomer conversion kinetics, the formation kinetics of the different dimers and oligomers were found similar for the HRP and PRX34 peroxidase. After a global comparison of the results obtained in homo- and copolymerization conditions, we examine in detail the PRX34-catalyzed copolymerization of S and G alcohols in order to dissect the whole mechanism recruited in the first steps of lignin synthesis.

2.3. Homopolymerization and copolymerization context: a bulk versus an endwise polymerization mechanism

Peroxidase-catalyzed oxidation of S or G alcohols allows to recover a soluble fraction of dimers and oligomers (PD $\leqslant$ 12; Fig. 3) that was analyzed for equivalent molar mass distribution by high performance size-exclusion chromatography (HPSEC). After an organic-solvent extraction, HPSEC profiles of the G alcohol products (Fig. 3a) and of the S and G alcohols copolymerization products

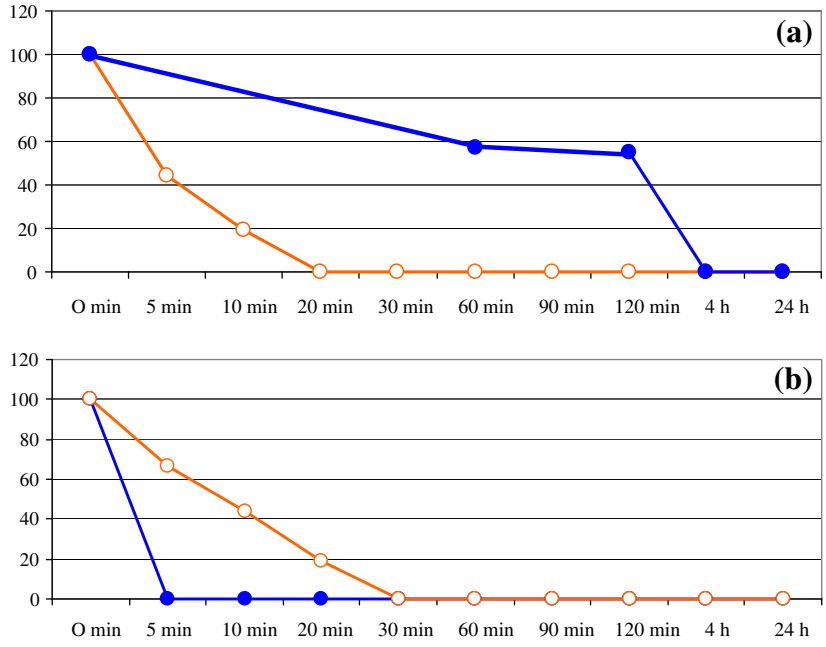

Fig. 2. PRX34-catalyzed oxidation kinetics of (●) S alcohol and (○) G alcohol under (a) homopolymerization (S or G alone) and (b) copolymerization (50/50 mol/mol S/G mixture) conditions. Relative weight contents determined by LC-PDA are normalized with respect to the initial alcohol content. Chromatographic conditions: C_{18} column (Highpurity, Thermo Electron Corporation, 5 µm, 150 × 4.6 mm) eluted with a 12–95 vol.% aqueous acetonitrile, 1‰ HCOOH gradient (45 min) and 1 ml min^{-1} flow rate; PDA signal 190–600 nm.

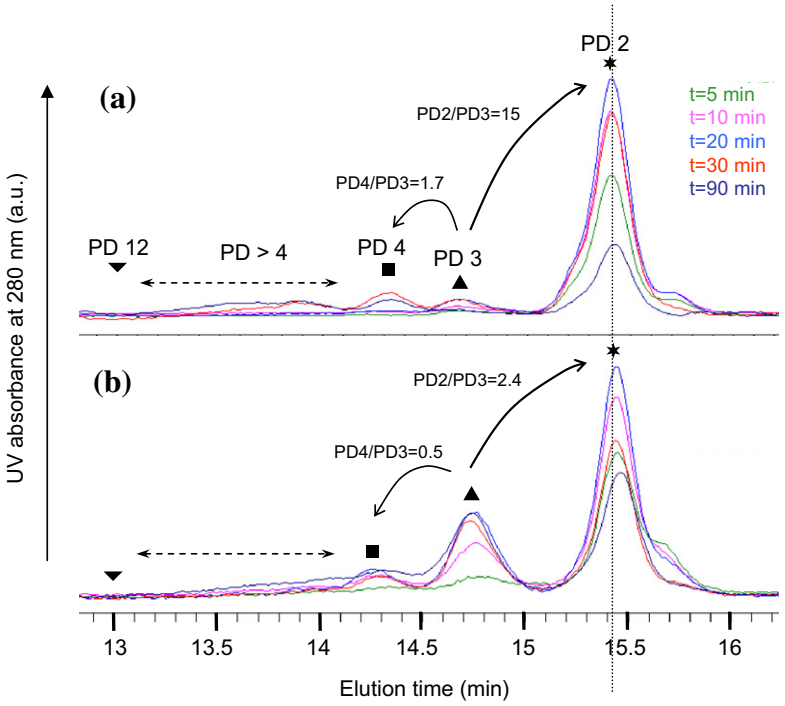

Fig. 3. Time-dependant variations of the HPSEC-PDA profiles of the PRX34-catalyzed oxidation products in (a) homopolymerization (G) and (b) copolymerization (S + G) conditions. The relative proportions of dimers (PD2) and tetramers (PD4) with respect to trimers (PD3) are estimated from the area of the corresponding elution peaks. Chromatographic conditions: PL-Gel column (5 µm; 100 Å; 4.5 × 600 mm; Polymer Laboratories) eluted with stabilized THF (1 ml min^{-1} flow rate); signal at 280 nm normalized with respect to the internal standard.

(Fig. 3b) revealed two distinct global polymerization patterns. Formation of dimers and oligomers is often described as resulting from radical couplings between two dehydrogenated compounds, either the oxidized monomer and the growing polymer phenoxy radical (endwise polymerization) or two oligomer phenoxy radicals (bulk polymerization) (Brunow et al., 1998). The two patterns observed here are typified by the respective proportion of odd- and even-PD oligomers. Although no absolute quantification is possible by SEC due to heterogeneity in the fractions corresponding to each PD, the height ratio between elution peaks can be used for comparative purpose to evaluate the relative proportion of these different fractions. In our case, the result was that homopolymerization led

to a higher proportion of dimers and tetramers, with respect to trimers, than copolymerization. Homopolymerization leads to a 6-fold higher dimer-to-trimer ratio (15 versus 2.4; Fig. 3) and a 3.4-fold higher tetramer-to-dimer ratio (1.7 versus 0.5; Fig. 3). The predominance of even-PD compounds in the absence of S monomers indicate a bulk polymerization process based on the coupling between dehydrodimers (Syrjanen and Brunow, 2000). On the other hand, the presence of odd-PD compounds in S–G copolymerization conditions suggests an endwise process based on couplings between the oxidized monomer and the elongating oligomer. These results show, in our *in vitro* oxidation conditions, that the presence of S monomers is enough to convert the polymerization of G monomers from a bulk to an endwise process.

In a previous paper (Méchin et al., 2007), we highlighted the importance of peroxidase availability on the orientation towards a bulk or an endwise polymerization process. Here, we underline the importance of the available monomers to also direct the polymerization process. Taking into account (i) the low peroxidase-catalyzed oxidation rate of S monomer in spite of its high potential reactivity (Tobimatsu et al., 2008c) and (ii) the low reactivity of S-type QM (Tobimatsu et al., 2008b) as proposed by these authors, G monomer may be involved in both transferring its radical to S monomer and quenching the stable S-type QM. The stability of S-type QM may result from the reduced positive charge density at the α-position because of the presence of two electron-donating OCH_3 groups (Tobimatsu et al., 2010). Thus, when considering a copolymerization context, G monomer first transfers its radical to S monomer allowing the formation of SS QM. This QM being stable, it is necessary that G monomer intercedes again to displace the equilibrium and to allow the polymerization to go further. These successive steps can explain that the polymerization process is slower with a mixture of S and G alcohols than with G alcohol alone. Such a slowing down of the polymerization process can explain the switch from a bulk to an endwise mechanism when adding S alcohol in the system.

This point is of importance when dehydrogenative polymerization product (DHP) synthesis has the objective to modelize lignifications in angiosperm where both G and S alcohols are incorporated.

2.4. Dissection of the mechanism recruited in the first steps of a PRX34-catalyzed copolymerization of S and G alcohols

Very schematically and according to Fig. 2b, the kinetics of oligomerization of the S–G mixture exhibit three distinct phases: the first one (0–5 min) corresponds to the presence of both S and G monomers; the second one (5–30 min) to the presence of G monomer only and the last one (30 min–24 h) to the absence of monomers.

In the first phase, dimers accumulation is very fast within the first 5 min reaction, and coincides with the S alcohol consumption rate (Fig. 4a). This coincidence is in agreement with the fact that the two main dimers formed, one SS homodimer and one SG heterodimer, involve S units. The SS dimer corresponds to a syringaresinol structure (ββ bond, Fig. 5) and the SG dimer corresponds to a phenyl coumaran (β5 bond, Fig. 6). After 5 min, all the S monomers are consumed.

During the second phase, the SS dimer content starts to decrease as soon as there are no S monomers left (Fig. 5). Meanwhile, G alcohol continues to be consumed during the next 25 min until total conversion (Fig. 4a). In agreement with the absence of S monomers after 5 min, SG dimer formation is no more observed beyond this reaction time (Fig. 6). G is then involved in the elongation of the existing S-based dimers and, in parallel, to the formation of G ββ, β5 and, to a lower extent, of β-*O*-4 homodimers. β-*O*-4 coupling between the G radical and the SS and SG dimers explain the formation of trimers 614 (614 is the molecular weight of

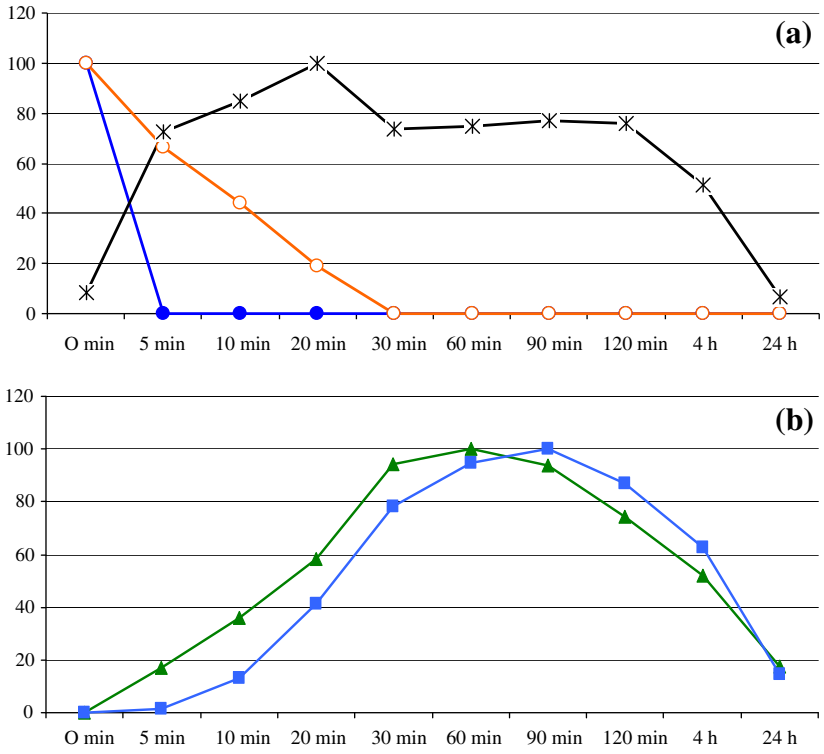

Fig. 4. PRX34-catalyzed oxidation kinetics of a 50/50 mol/mol S/G mixture showing (a) the coincidence of the monomer consumption, (●) S alcohol and (○) G alcohol, with the total dimer (*) formation and (b) the slight time shift but similar profiles between the total (▲) trimers and (■) tetramers formation curves. Relative weight contents determined by LC-PDA are normalized with respect to the maximal content of each species. Chromatographic conditions: C_{18} column (Highpurity, Thermo Electron Corporation, 5 μm, 150 × 4.6 mm) eluted with a 12–95 vol.% aqueous acetonitrile, 1‰ HCOOH gradient (45 min) and 1 ml min^{-1} flow rate; PDA signal 190–600 nm.

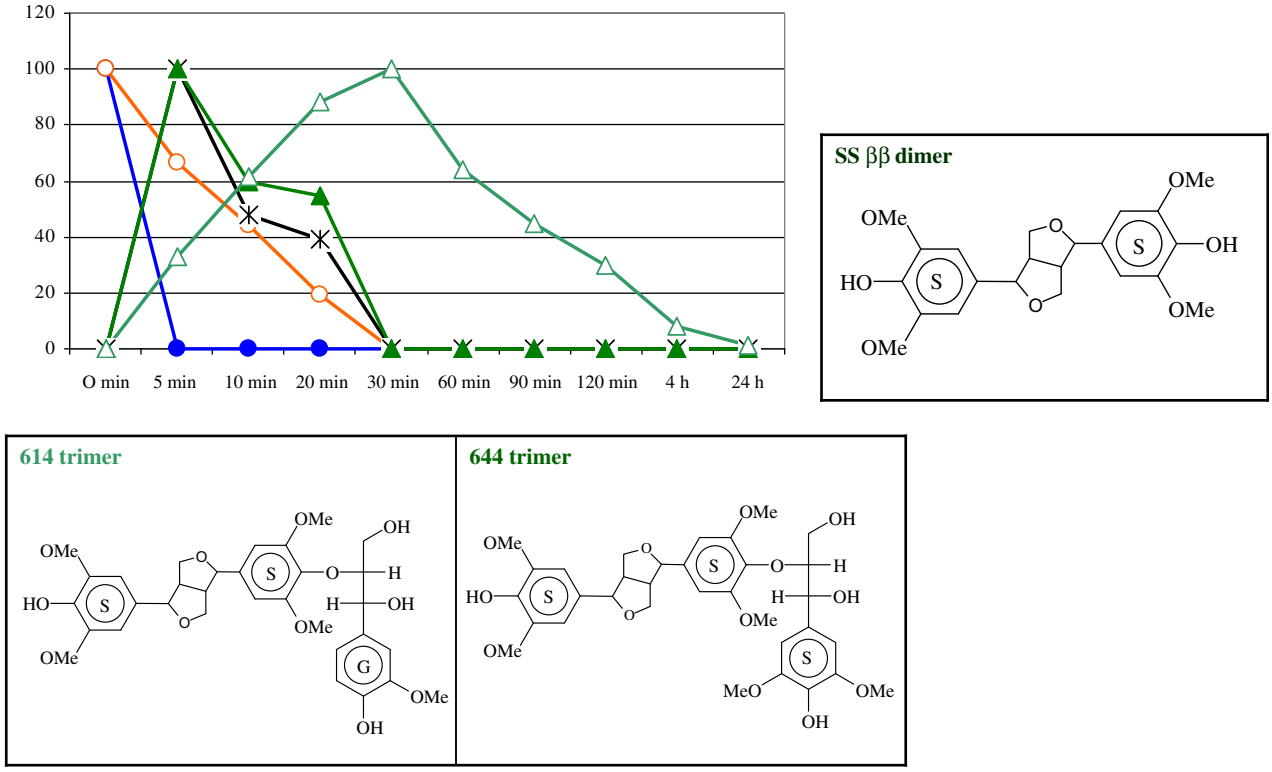

Fig. 5. PRX34-catalyzed oxidation kinetics of a 50/50 mol/mol S/G mixture showing the simultaneous formation of (*) the syringaresinol (ββ) S homodimer and (▲) the 644 SSS homotrimer and the delayed formation of (△) the 614 SSG heterotrimer. Both trimers are formed by a β-O-4 coupling between the syringaresinol structure and one monomer (G or S alcohol). Thirty minutes is a key reaction time corresponding to the total consumption of the (●) S and (○) G alcohol monomers, the S homodimers and the S homotrimers and to the maximum formation of the heterotrimer. Relative weight contents determined by LC-PDA (monomers and dimers) and LC-ESI-MS (trimers and tetramers) are normalized with respect to the maximal content of each species. Chromatographic conditions: C_{18} column (Highpurity, Thermo Electron Corporation, 5 µm, 150 × 4.6 mm) eluted with a 12–95 vol.% aqueous acetonitrile, 1‰ HCOOH gradient (45 min) and 1 ml min^{-1} flow rate; PDA signal 190–600 nm; negative ion ESI-MS spectra (120–2000 *m/z*) acquired using an ion trap spectrometer (Finnigan LCQ-DECA – Thermo Electron Corporation) setting the needle voltage at 4 kV and the desolvating capillary temperature at 350 °C.

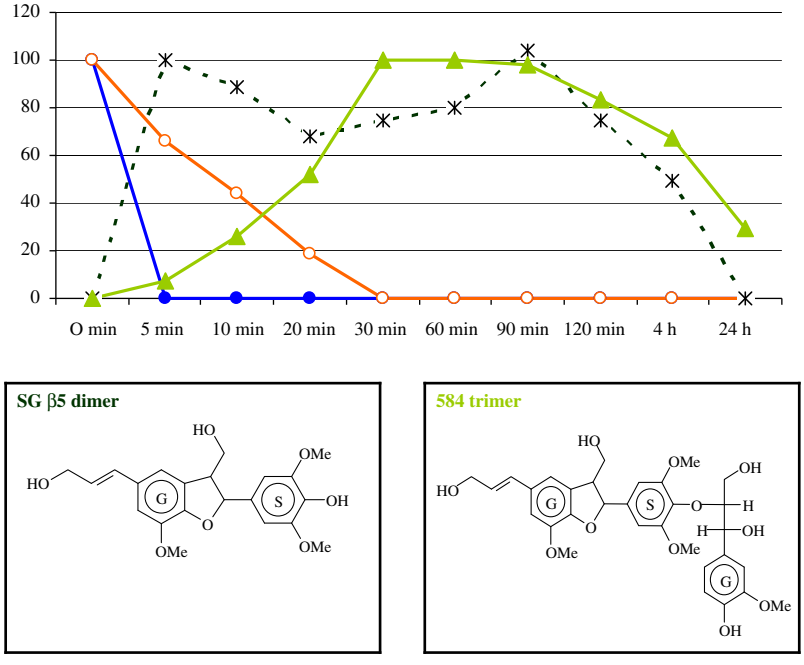

Fig. 6. PRX34-catalyzed oxidation kinetics of a 50/50 mol/mol S/G mixture showing the fast formation of the (*) β5 SG heterodimer symmetrically to the consumption of the (●) S alcohol and the delayed formation of the (▲) 584 SGS heterotrimer symmetrically to the consumption of the (○) G alcohol. Relative weight contents determined by LC-PDA (monomers and dimers) and LC-ESI-MS (trimers) are normalized with respect to the maximal content of each species. Chromatographic conditions: C_{18} column (Highpurity, Thermo Electron Corporation, 5 µm, 150 × 4.6 mm) eluted with a 12–95 vol.% aqueous acetonitrile, 1‰ HCOOH gradient (45 min) and 1 ml min^{-1} flow rate; PDA signal 190–600 nm; negative ion ESI-MS spectra (120–2000 *m/z*) acquired using an ion trap spectrometer (Finnigan LCQ-DECA – Thermo Electron Corporation) setting the needle voltage at 4 kV and the desolvating capillary temperature at 350 °C.

the formed trimer and will be used elsewhere to mention this specific trimer) and 584 (584 is the molecular weight of the formed trimer and will be used elsewhere to mention this specific trimer) respectively (Figs. 5 and 6 and Supplementary material). The 644 trimer (644 is the molecular weight of the formed trimer and will be used elsewhere to mention this specific trimer) is an analogous of the 614 trimer formed by a β-*O*-4 coupling between a S unit and the SS dimer (Supplementary material). Very interestingly, the G homodimers did not lead to any trimers, which show the higher reactivity of the S-based structure towards copolymerization. According to the respective dimer conversion rate, the SS β–β structure turns out to be the most reactive one. The 5 min delay by which tetramers appear after trimers (Fig. 4b and Supplementary material) indicate that the tetramers are formed by elongation of the trimer by a monomer, according to an endwise process, and not by homocoupling between dimers. The structure of the 810 and 840 tetramers (810 and 840 are the molecular weights of the formed tetramers and will be used elsewhere to mention these specific tetramers) confirm that they might be formed from the 614 and 644 trimers by elongation with one G unit, respectively (Fig. 7). Here again, elongation proceeds by β-*O*-4 linkages. We found no tetramer derived from the 584 trimer, which suggests that the endwise elongation is favoured by the presence of one terminal S structure. In parallel to this endwise elongation process a bulk-type process seems to occur, involving the GG β–β homodimer. Indeed, whereas no corresponding trimer or tetramer was observed, we detected some pentamers with molar mass of 970 g mol^{-1}. This mass corresponds exactly to the coupling between a GG homodimer and the 614 trimer and excludes the involvement of a β-*O*-4 bond for this coupling. In view of the structure of the SSG trimer and GG dimer, the coupling possibilities are the biphenyl or biphenyl ether one.

The third phase begins when all G units are consumed (Fig. 4a). Amazingly, trimers and tetramers are apparently still produced until 60–90 min, although there is no monomer left for endwise elongation. This apparent increase in trimer and tetramer content can be explained by some structural modification within the reaction mixture. Indeed, at 30 min, trimers and tetramers of a new type start to be produced, whereas there is no monomer available anymore for the synthesis of trimer or tetramers. The mass spectra of these compounds (characteristic fragments at *m/z* 433 and 629 respectively) suggest that they could correspond to the speculative structures incorporating a sinapaldehyde (S′) unit and proposed by Morreel et al. (2004). These structures are trimers (compound 31 GSS′ or GS′S; Morreel et al. (2004) and Supplementary material) and tetramers (compound 35 GGSS′ or GGS′S;

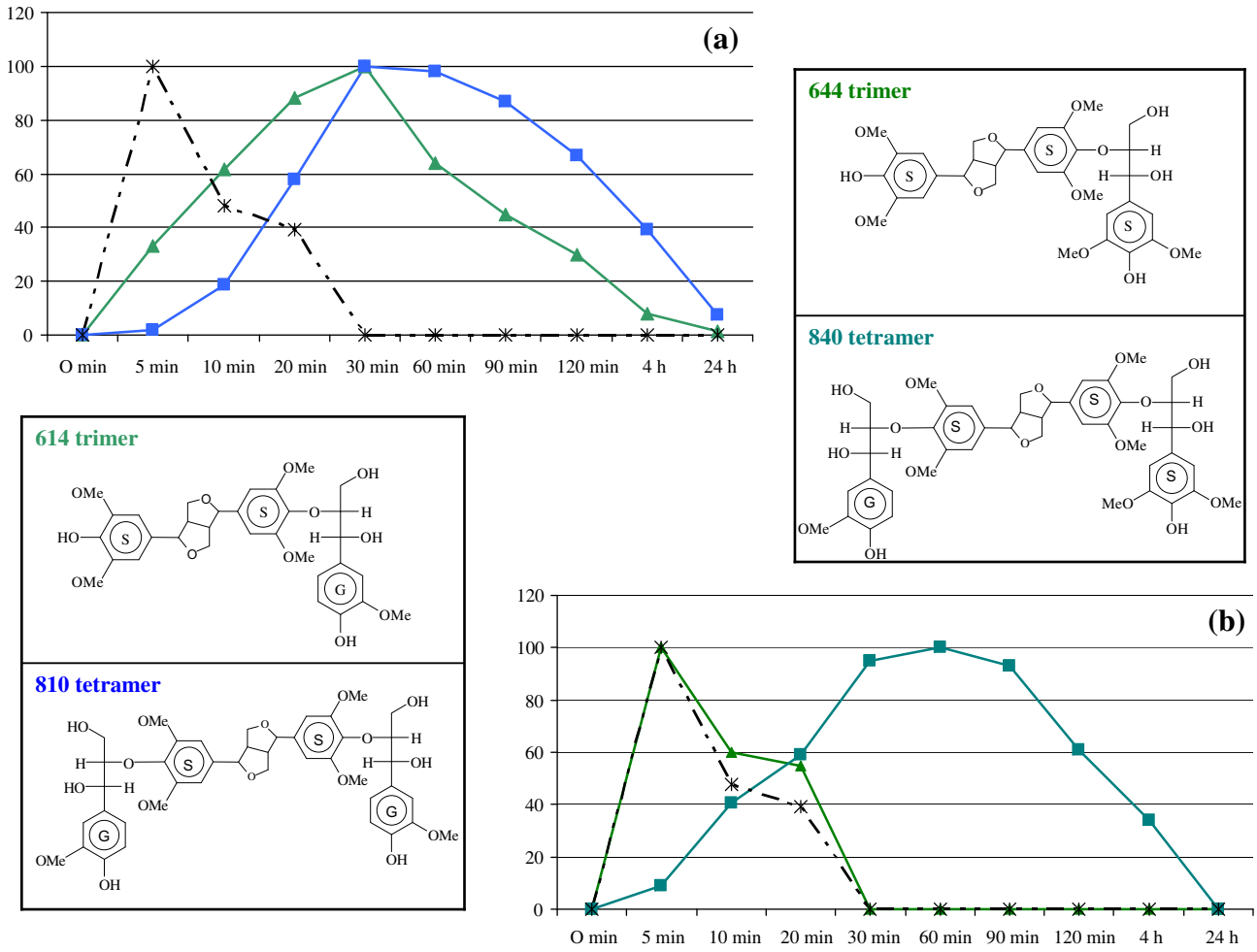

Fig. 7. PRX34-catalyzed oxidation kinetics of a 50/50 mol/mol S/G mixture showing the formation of the two tetramers (a; ■) 810 GSSG and (b; ■) 840 GSSS. The formation curve of the 840 tetramer parallels the consumption curve of the (b; ▲) 644 trimers whereas the 810 tetramer formation curve follows the same shape as the (a; ▲) 614 trimer. Both tetramers reach their maximum formation at 30 min. Relative weight contents determined by LC-ESI-MS (trimers) are normalized with respect to the maximal content of each species. Chromatographic conditions: C_{18} column (Highpurity, Thermo Electron Corporation, 5 μm, 150 × 4.6 mm) eluted with a 12–95 vol.% aqueous acetonitrile, 1‰ HCOOH gradient (45 min) and 1 ml min^{-1} flow rate; PDA signal 190–600 nm; negative ion ESI-MS spectra (120–2000 *m/z*) acquired using an ion trap spectrometer (Finnigan LCQ-DECA – Thermo Electron Corporation) setting the needle voltage at 4 kV and the desolvating capillary temperature at 350 °C.

Morreel et al. (2004) and Supplementary material) involving one sinapaldehyde unit linked with S alcohol. According to these authors, these structures may result from the incorporation of a sinapaldehyde unit during the oligomerization process. In our study, the maximum contents of these two compounds are reached at 60 for the trimer and at 90 min for the tetramers (Fig. 8). The progressive accumulation of GSS′ and GGSS′ observed in our kinetic approach at later stages (Fig. 9), together with the absence of aldehydic structures of smaller PD suggest that these unauthenticated structures may result from the oxidation of a pre-existing oligomer rather than from the direct incorporation of a sinapaldehyde monomer.

Also during this third phase, the consumption of the GG β5 dimer is observed together with the appearance of a series of oligomers of PD > 5. Most of these oligomers include a pentameric sequence corresponding to an ion of 969 amu. This sequence can be explained by the cross-coupling between the 584 GSG trimer and the 388 GS dimer or between a 358 GG dimer and the 810 GSSG tetramer with a fragmentation of the resulting oligomer by cleavage of the end-sequence β-*O*-4 S–G bond. The highest DP oligomer fragment detected exhibits a *m/z* of 1972 amu, which corresponds theoretically to a decamer sequence involving six G monomers, four S monomers and four β-*O*-4 bonds. This fragment is accompanied on the same mass spectrum by a series of fragments which we suspect to stem from an oligomer of PD 12 (Fig. 9). We propose for this oligomer a sequence which respect both the mass of the fragments observed and the structure of the oxidation products available at the time when these oligomers start to be detected (Fig. 10; 90 min). Thus, the oligomer can tentatively be assigned to a structure resulting from the coupling between two 584 GSG trimers, one 810 GSSG tetramer and one 358 GG dimer. The 584 GSG trimer, which does not take part to any endwise elongation process and remains unreactive during the first 90 min (Fig. 10), would then be recruited in the very last stage of the kinetics once other more reactive species are already consumed. The lower reactivity of the 584 trimer compared to 644 and 614 trimers could be explained by the fact that S species are always more reactive. Thus, the more S units are involved in the structure, the most reactive this structure appears. Given the far highest consumption rate of the ββ GG dimer compared to its β5 analogue (Fig. 10), it is most probable that the 358 dimer present in the PD > 4 sequence is the ββ one.

To summarize, the PRX34-catalyzed oxidation of a 50/50 mol/mol S/G mixture leads mainly to four dimers (1 SS ββ, 1 SG β5, 1 GG β5 and 1 GGββ), three trimers (1 SSS, 1 SSG and 1 SGG), two tetramers (1 SSSG, 1 GSSG) and a series of oligomers of PD > 4. The successive formation and consumption of all these compounds along the oxidation reaction is schematized in Fig. 10. Such a scheme is particularly useful to understand how a given oligomer sequence can be formed at a given reaction time. For instance, it allowed us to exclude an endwise elongation mechanism for the formation of the PD > 4 oligomers since they are no monomer left after 30 min, time at which the PD > 4 oligomers starts to appear. The scheme also helps to illustrate the respective reactivity of the different species as a function of the composition of the reaction medium. The four dimers identified are precisely the one identified by Kishimoto et al. (2010) after thioacidolysis of a polymeric fraction of Zutropf DHPs synthesized also from an equimolar S/G alcohols mixture. These authors found a molar ratio between the thioacidolysis dimers in favour of the SS syringaresinol dimer (GG/GS/SS = 27/23/50). The SSS trimer and the corresponding SSSG tetramer were the major oligomers identified by Evtuguin and Amado (2003) in the low-molar-mass fraction of *Eucalyptus globulus* dioxane lignin, together with a SGSSG pentamer that corre-

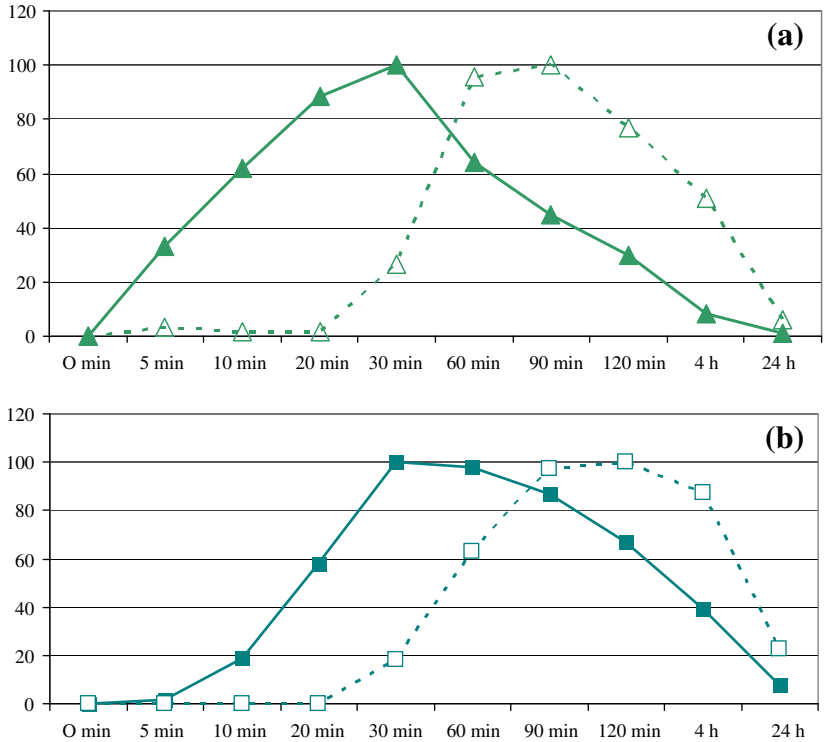

Fig. 8. PRX34-catalyzed oxidation kinetics of a 50/50 mol/mol S/G mixture showing the similar shift between the formation curves of the (a; ▲) 614 trimer and the (b; ■) 810 tetramer and the speculative aldehydic structures (a; S′SG △) and (b; GS′SG □). Relative weight contents determined by LC-ESI-MS are normalized with respect to the maximal content of each species. Chromatographic conditions: C_{18} column (Highpurity, Thermo Electron Corporation, 5 μm, 150 × 4.6 mm) eluted with a 12–95 vol.% aqueous acetonitrile, 1‰ HCOOH gradient (45 min) and 1 ml min^{-1} flow rate; PDA signal 190–600 nm; negative ion ESI-MS spectra (120–2000 *m/z*) acquired using an ion trap spectrometer (Finnigan LCQ-DECA – Thermo Electron Corporation) setting the needle voltage at 4 kV and the desolvating capillary temperature at 350 °C.

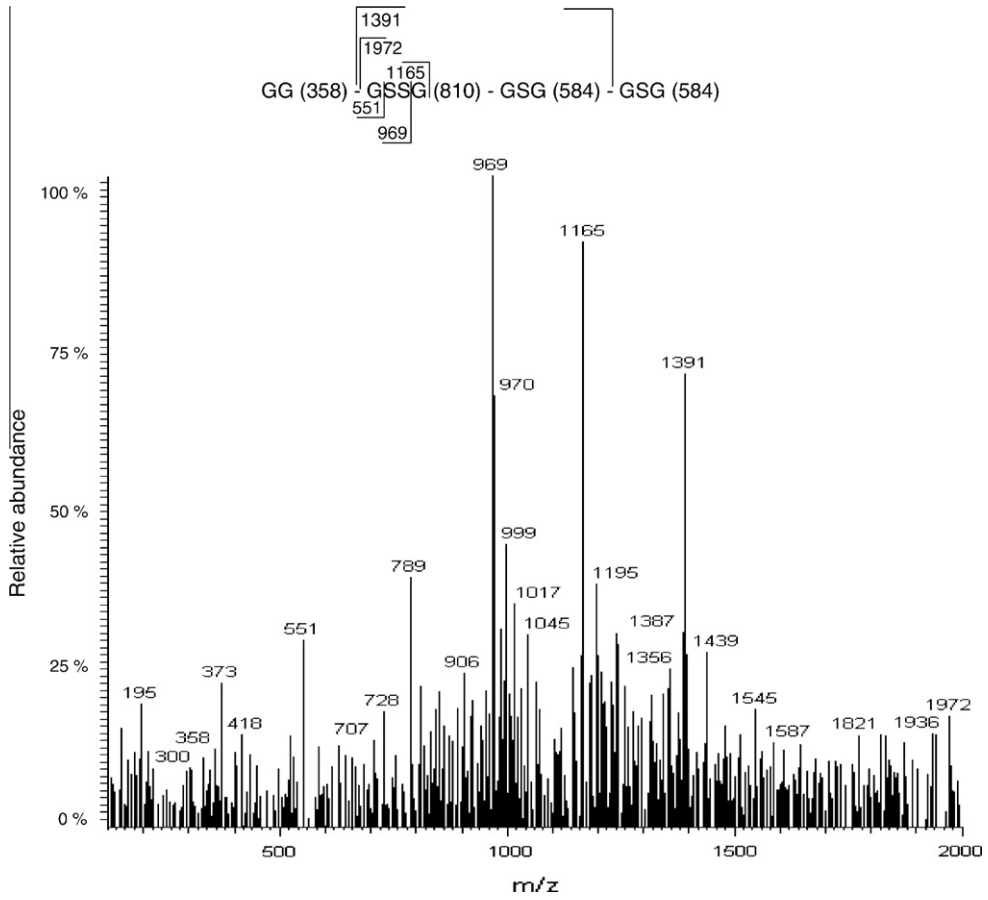

Fig. 9. ESI-MS spectrum (elution time: 15.91 min, S–G copolymerization mixture recovered at 90 min) showing fragments that can be tentatively assigned to structural sequences derived from an oligomer of PD 12 (fragments corresponding to PD > 10 cannot be detected given the 120–2000 amu *m*/*z* scan range of the spectrometer). The sequence of these oligomers is in agreement with their formation by coupling of the lower PD oligomer present in the oxidation mixture at their time when they appear.

sponds to the GSSG tetramer coupled with a S monomer (data not shown). The more complex poplar xylem extract analyzed by et al. (2004) also comprises all the dimers, trimers and tetramers identified here, including the speculative aldehyde analogues. No oligolignol of PD > 4 could be detected by the authors.

3. Conclusions

The objectives of this study were simultaneously to test the activity of a class III peroxidase purified for the first time from *A. thaliana* and to use this plant-purified enzyme to dissect the oligomerization mechanisms of two main precursors of lignin, G and S alcohols. We not only confirmed that the PRX34 peroxidase can initiate the oxidation-catalyzed oligomerization of an equimolar S/G mixture but also demonstrate that its *in vitro* activity is identical to that of the HRP. This similarity could be explained from the high sequence homology (94%) observed between those two proteins. As for HRP, the PRX34 shows a high substrate specificity and seems unable to directly oxidize S monomers.

By monitoring the oxidation of a mixture of S and G alcohol in comparison with the oxidation of S or G alcohol alone, we succeed in evaluating the polymerization mode recruited in each condition. We show that the presence of S monomers converted the polymerization of G monomers from a bulk to an endwise mechanism. We also confirm the role of G alcohol as radical mediator and identify key structures associated with the incorporation of S alcohol. This study brings new information on the compared reactivity of S and S/G lignin model compounds and is supposed to provide some precious information to better apprehend the complex lignification process in plants. S-type lignins in plants, such as eucalyptus lignin are known to be associated to higher β-*O*-4 contents. We show here that the β-*O*-4 bonds are incorporated into the polymer as soon as the trimerization step and that the formation of such bonds is initiated by the presence of syringaresinol homodimer.

Most of the oligomers identified in the run of our *in vitro* S–G copolymerization have been identified also in the oligomer fraction recovered from plant extracts. This shows that *in vitro* polymerization remains a useful and reliable tool to investigate the polymerization mechanisms of lignin. A specificity of our study was to implement a mechanistic approach through a kinetic investigation. This kinetic investigation of the very first steps of oligomerization not only informs us on the respective reactivity of the different structures, but also provides a way to monitor the sequential formation of the different oligomers. Based on our results, we propose a general scheme for S–G copolymerization. We observe that an endwise and a bulk mechanisms are likely to co-exist within the same system, the bulk mechanisms occurring after total consumption of the monomers. Even if lignification is a continuous process in plant cell wall, although not very frequent, it can be imagined that such a situation of monomer starvation in plants could occur at specific stages of plant development and/or in specific tissues, which could also account for the spatiotemporal variability of lignin structure. Results obtained in this study could be completed in the future by an equivalent approach taking into account the continuous process of lignification in plant cell wall and thus operating in Zutroph mode rather than Zulauf mode.

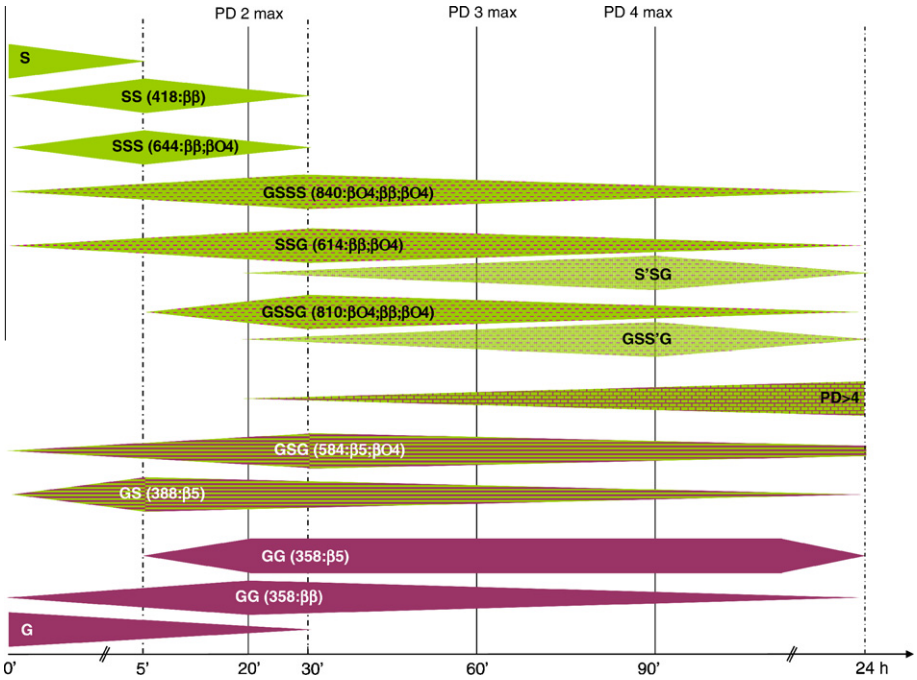

Fig. 10. General schematic representation of the formation and consumption kinetics of the different species identified in the PRX34-catalyzed oxidation medium from a 50/50 mol/mol S/G mixture: (S) S alcohol; (G) G alcohol; (SS 418 ββ) S syringaresinol homodimer; (SSS 644:ββ;βO4) S homodimer derived from the syringaresinol dimer; (GSSS 840:βO4;ββ;βO4) heterotetramer derived from the S homotrimer; (SSG 614:ββ;βO4) heterotrimer derived from the syringaresinol dimer; (S′SG) speculative heterotrimer aldehyde; (GSSG 810:βO4;ββ;βO4) heterotetramer derived from the SSG heterotrimer, (GS′SG) speculative heterotetramer aldehyde; (GG 358 ββ) G pinoresinol homodimer; (GG 358 β5) G phenyl coumaran homodimer and (GS 358 β5) its heterodimer analogue; (GSG 584:β5;βO4) heterotrimer derived from the GS β5 dimer; (PD > 4) heterooligomers of polymerization degree higher than 4 derived only from dimers, trimers and tetramers present in the mixture at 30 min (at this reaction time, no monomer are anymore available for an elongation through an endwise mechanism).

4. Experimental

4.1. Plant material

The ecotypes Wassilewsija (WS) and Columbia (ColO) were used in this work. Two homozygous lines were used for PERX 34 overproducing. Wild type or mutant was identified in the *A. thaliana* collection of Versailles (Bouche and Bouchez, 2001) and in the Salk Institute Genomic Analysis Laboratory (Alonso et al., 2003). The Atprx34 line was selected using systematic border sequencing program of the Salk Institute (San Diego, USA) on TAIR site.

A construct including cDNA of PRX34 (clone WS Versailles collection) under the control of CaMV35S promotor and fusionned with GFP (codon stop in-phase) was performed using the gateway binary vector (pGWB5, Invitrogen). The transformed and the wild type lines were grown together in greenhouse to ensure uniform environmental conditions. Stems (5–6 weeks-old) were harvested and used for peroxidase purification.

4.2. Purification of PRX34 A. thaliana peroxidase

Approximately 7 g of Arabidopsis stems were blended for 5 min, suspended in 7 ml of extraction buffer (25 mM BisTris (pH 7), 200 mM $CaCl_2$, 10% (v/v) glycerol, 4 μM Na-cacodylate and 1/200 (v/v) protease inhibitor cocktail (P-9599; Sigma)) and blended 5 min. The material was centrifuged twice at 8 °C for 5 min at 3000*g* and one time at 4 °C for 5 min at 13,000*g*. The supernatant was additionally centrifuged at 8 °C for 45 min at 15,000*g*. The protein purification was performed in two steps:

(i) Affinity chromatography on a 0.5 × 3 cm column filled with 1 ml of Concanavalin-A Sepharose (Sigma) and washed with 3 ml of 20 mM Tris–HCl, 0.5 M NaCl buffer (pH 7.4). The soluble protein extract was loaded and the column washed with 10 ml of buffer. The proteins were eluted with 0.2 M methyl-α-glucopyranoside in the same buffer. The eluates were collected (1 ml per fraction) and 3 or 5 μl samples from each fraction were tested for peroxidase activity. Pooled fractions showing peroxidase activity were equilibrated in 25 mM Tris–HCl buffer (pH 7.4) containing 5% glycerol (v/v) and 0.015% Triton X-100 (v/v). Glycerol was added to the buffer to prevent the partial enzymatic inactivation.

(ii) *Cation exchange chromatography:* The soluble protein extract was loaded on a CM-Sepharose (Sigma) cation exchange column (1.5 × 2.5 cm). The proteins were eluted with the same buffer, first alone and then with a 0.0–0.5 M NaCl discontinuous gradient using 2 ml of NaCl solution, increasing by 0.025 M. One-ml fractions were collected and 3 or 5 μl assayed for peroxidase activity.

4.3. Identification of purified peroxidase by Maldi-TOF MS

In order to identify the gene sequence of the Per34, the 44.7 kDa protein band observed in the SDS–PAGE gel was in-gel digested with 0.5 μg of trypsin (Gold, Promega) over-night. The peptides were extracted with 2 × 0.1 trifluoro acetic acid (TFA) in acetonitrile/25 mM ammonium carbonate buffer (60/40, v:v) and concentrated. The matrix solution contained 0.3 g/l of 4-hydroxy-α-cyanocinnamic acid in ethanol/acetone (2/1, v:v).

Equal volumes of purified peptides sample or calibration standard (peptide calibration mixture Pepmix 1, LaserBio Labs, Sophia Antipolis, France) were mixed with the matrix solution. One μl of this matrix/sample mixture was applied onto the target and let to dry at room temperature.

Mass spectra were acquired on a Bruker Reflex III MALDI-TOF instrument equipped with a nitrogen laser with an emission wave-

length of 337 nm. Spectra were obtained in the reflectron mode at an accelerating voltage of 19 kV. FlexAnalysis software was used for data analysis.

Proteins were identified on the using peptide mass fingerprints and Mascot interface (http://www.matrixscience.com/) in May 2007. The *A. thaliana* database was queried, with no more than one missed cleavage.

4.4. In vitro peroxidase activity assays

A 20 mg ml^{-1} solution of the substrate 3,3′,5,5′-tetramethylbenzydine (TMB) was prepared in DMSO, and stored in aliquots at −20 °C.

The reaction mixture contained 100 mM acetate citric acid buffer (pH 6), 0.4 µl of 6% (w/v) H_2O_2, 4 µl TMB and 1–3 µl of protein extract in a total volume of 800 µl. The reaction was carried out at room temperature for 1 min and stopped by the addition of 30 µl concentrated H_2SO_4 to the assay mixture. The TMB oxidation was monitored by the increase of absorbance at 450 nm.

4.5. SDS–PAGE and protein gel blot analysis

Protein-denaturating SDS–PAGE was carried out using 10% polyacryamide gels. Standard markers (molecular range 15–100 kDa; Sigma) were used to determine the approximate molecular masses of purified proteins in silver stained gels.

Proteins were transferred onto 0.45 µm Hybond ECL membrane (Amersham Biosciences, Piscataway, NJ) by electroblotting. Protein detection was performed using first polyclonal antibodies raised against peroxidases (Buffard et al., 1990) and second antibodies phosphatase alkaline conjugate.

4.6. Oxidative coupling of coniferyl (G) and sinapyl (S) alcohols

G and S alcohols were kindly synthesized by Dr. B. Cathala, according to the method of Ludley and Ralph (1996). The internal standard 3,4,5-trimethoxybenzoic acid (TMBA) was obtained from Fluka (Buchs, Switzerland) and hydrogen peroxide (30 wt.% solution) from Acros (New Jersey). Horseradish peroxidase type II (HRPII, 180 U/mg) was purchased from Sigma Chemical Co. (St. Louis, MO). Phosphate buffer was prepared from sodium dihydrogen phosphate ($NaH_2PO_4{\cdot}2H_2O$) and di-sodium hydrogen phosphate ($Na_2HPO_4{\cdot}2H_2O$) (analytical reagents; Prolabo, France). The 3,3′,5,5′-tetramethylbenzydine substrate (TMB) was purchased from Sigma (St. Louis, MO, USA).

These oxidative coupling experiments were carried out at a microscale level according to a modified version of Fournand and Lapierre (2001). An internal standard of 2 mM TMBA (800 µl) in 10 mM NaH_2PO_4–Na_2HPO_4, pH 5.5, buffer was added to 1600 µl of 2 mM G alcohol, S alcohol or a mixture 50/50 of both G and S alcohols in the same buffer. A solution of 4 mM hydrogen peroxide (800 µl) in ultrapure water was then added before the addition of 1600 µl of a 50 ng/ml solution of horseradish peroxidase type II in the 10 mM NaH_2PO_4–Na_2HPO_4, pH 5.5, buffer or a solution of purified *A. thaliana* PRX34 peroxidase in the 10 mM NaH_2PO_4–Na_2HPO_4, pH 5.5, buffer. A reference was made by replacing peroxidase solution by 10 mM NaH_2PO_4–Na_2HPO_4, pH 5.5, buffer. Mixtures were kept at 30 °C, and aliquots of the oxidation reaction medium (600 µl) were regularly taken, mixed with HCl 0.1 N and extracted with a 50/50 v/v dichloromethane/ethyl acetate mixture before evaporation of the organic phase to dryness.

4.7. Size-exclusion chromatography (SEC) analysis of oligomeric products

The extracted soluble fractions were analyzed by SEC, using a PL-Gel column (Polymer Laboratories, 5 µm, 100 Å, 600 × 7.5 mm) with tetrahydrofuran (THF) as an eluent (stabilized THF, JT Baker; 1 ml min^{-1}) and 280 nm UV detection. The polymerization degrees (PD) were assigned according to the apparent molar masses of the compounds based on a calibration with polyethylene oxide standards (Igepal, Aldrich) and purified lignin model compounds (Baumberger et al., 2003).

4.8. LC/MS analysis of oligomeric products

The extracted soluble fractions were analyzed by reverse-phase LC with electro spray ionisation (ESI)-MS and photodiode array (PDA) co-detection. The methanolic solutions were ultra filtrated (0.45 µm – GHP Acrodisc – Gelman) and injected on a C_{18} column (Highpurity, Thermo Electron Corporation, 5 µm, 150 × 4.6 mm) using a 12–95 vol.% aqueous acetonitrile, 1‰ HCOOH gradient (45 min) and 1 ml min^{-1} flow rate. Negative ion ESI-MS spectra (120–2000 *m/z*) were acquired using an ion trap spectrometer (Finnigan LCQ-DECA – Thermo Electron Corporation) setting the needle voltage at 4 kV and the desolvating capillary temperature at 350 °C. The synthesized products were assigned according to their PDA (190–600 nm) and mass spectra as reported by Morreel et al. (2004). The polymerization degree and amount of β-*O*-4 bonds of the oligomers were determined according to the mass of the deprotonated ion.

Acknowledgements

The authors sincerely acknowledge Dr. Bernard Cathala for his help in synthesizing G and S monomers, François Perreau on the Plateau Technique Spécifique de Chimie du Végétal of IJPB for Maldi-TOF analyses and Dr. Paul-Henri Ducrot for his critical reading of the manuscript and fruitful discussions.

The LC-MS equipment was obtained from a common financial support of INRA and Région Ile de France (SESAME Grant).

This work was funded by the French Research National Agency (ANR) in the context of the MAGIC program (ANR-08-BLAN-0307).

Appendix A. Supplementary data

Supplementary data associated with this article can be found, in the online version, at doi:10.1016/j.phytochem.2010.06.011.

References

Alonso, J.M., Stepanova, A.N., Leisse, T.J., Kim, C.J., Chen, H., Shinn, P., Stevenson, D.K., Zimmerman, J., Barajas, P., Cheuk, R., Gadrinab, C., Heller, C., Jeske, A., Koesema, E., Meyers, C.C., Parker, H., Prednis, L., Ansari, Y., Choy, N., Deen, H., Geralt, M., Hazari, N., Hom, E., Karnes, M., Mulholland, C., Ndubaku, R., Schmidt, I., Guzman, P., Aguilar-Henonin, L., Schmid, M., Weigel, D., Carter, D.E., Marchand, T., Risseeuw, E., Brogden, D., Zeko, A., Crosby, W.L., Berry, C.C., Ecker, J.R., 2003. Genome-wide insertional mutagenesis of *Arabidopsis thaliana*. Science 301, 653–657.

Aoyama, W., Sasaki, S., Matsumura, S., Mitsunaga, T., Hirai, H., Tsutsumi, Y., Nishida, T., 2002. Sinapyl alcohol-specific peroxidase isoenzyme catalyzes the formation of the dehydrogenative polymer from sinapyl alcohol. J. Wood Sci. 48, 497–504.

Barcelo, A.R., Ros, L.V.G., Carrasco, A.E., 2007. Looking for syringyl peroxidases. Trends Plant Sci. 12, 486–491.

Baumberger, S., Fournand, D., Pollet, B., Lapierre, C., Ducrot, P.-H., 2003. Peroxidase-catalyzed polymerization of monolignols: HPSEC investigation of the oligomerization step. In: Proceedings of the 12th ISWPC, Madison, pp. 165–168.

Bouche, N., Bouchez, D., 2001. Arabidopsis gene knockout: phenotypes wanted. Curr. Opin. Plant Biol. 4, 111–117.

Brunow, G., Kilpelainen, I., Sipila, J., Syrjanen, K., Karhunen, P., Setala, H., Rummakko, P., 1998. Oxidative coupling of phenols and the biosynthesis of lignin. In: Lewis, N.G., Sarkanen, S. (Eds.), Lignin and Lignan Biosynthesis. American Chemical Society, Washington, DC, pp. 131–147.

Buffard, D., Breda, C., van Huystee, R.B., Asemota, O., Pierre, M., Ha, D.B., Esnault, R., 1990. Molecular cloning of complementary DNAs encoding two cationic peroxidases from cultivated peanut cells. Proc. Natl. Acad. Sci. USA 87, 8874–8878.

Evtuguin, D.V., Amado, F.M.L., 2003. Towards a better understanding of lignin assembly: the assessment of the sequential order of building blocks and inter-units linkages using electrospray ionisation mass spectrometry. In: Proceedings of the 12th ISWPC, Madison, pp. 277–280.

Fournand, D., Lapierre, C., 2001. Capillary zone electrophoresis of coniferyl alcohol oxidation products. J. Agric. Food Chem. 49, 5727–5731.

Fournand, D., Cathala, B., Lapierre, C., 2003. Initial steps of the peroxidase-catalyzed polymerization of coniferyl alcohol and/or sinapyl aldehyde: capillary zone electrophoresis study of pH effect. Phytochemistry 62, 139–146.

Freudenberg, K., Hubner, H.H., 1952. Hydroxycinnamyl alcohols and their dehydrogenation polymers. Chem. Ber. 85, 1181–1191.

Gabaldon, C., Lopez-Serrano, M., Pedreno, M.A., Barcelo, A.R., 2005. Cloning and molecular characterization of the basic peroxidase isoenzyme from *Zinnia elegans*, an enzyme involved in lignin biosynthesis. Plant Physiol. 139, 1138–1154.

Kishimoto, T., Chiba, W., Saito, K., Fukushima, K., Uraki, Y., Ubukata, M., 2010. Influence of syringyl to guaiacyl ratio on the structure of natural and synthetic lignins. J. Agric. Food Chem. 58, 895–901.

Ludley, F.H., Ralph, J., 1996. Improved preparation of coniferyl and sinapyl alcohols. J. Agric. Food Chem. 44, 2942–2943.

Marjamaa, K., Kukkola, E., Lundell, T., Karhunen, P., Saranpaa, P., Fagerstedt, K.V., 2006. Monolignol oxidation by xylem peroxidase isoforms of Norway spruce (*Picea abies*) and silver birch (*Betula pendula*). Tree Physiol. 26, 605–611.

Méchin, V., Baumberger, S., Pollet, B., Lapierre, C., 2007. Peroxidase activity can dictate the *in vitro* lignin dehydrogenative polymer structure. Phytochemistry 68, 571–579.

Minic, Z., Jamet, E., Negroni, L., der Garabedian, P.A., Zivy, M., Jouanin, L., 2007. A sub-proteome of *Arabidopsis thaliana* mature stems trapped on Concanavalin A is enriched in cell wall glycoside hydrolases. J. Exp. Bot. 58, 2503–2512.

Morreel, K., Ralph, J., Kim, H., Lu, F.C., Goeminne, G., Ralph, S., Messens, E., Boerjan, W., 2004. Profiling of oligolignols reveals monolignol coupling conditions in lignifying poplar xylem. Plant Physiol. 136, 3537–3549.

Nielsen, K.L., Indiani, C., Henriksen, A., Feis, A., Becucci, M., Gajhede, M., Smulevich, G., Welinder, K.G., 2001. Differential activity and structure of highly similar peroxidases. Spectroscopic, crystallographic, and enzymatic analyses of lignifying *Arabidopsis thaliana* peroxidase A2 and horseradish peroxidase A2. Biochemistry 40, 11013–11021.

Quiroga, M., Guerrero, C., Botella, M.A., Barcelo, A., Amaya, I., Medina, M.I., Alonso, F.J., de Forchetti, S.M., Tigier, H., Valpuesta, V., 2000. A tomato peroxidase involved in the synthesis of lignin and suberin. Plant Physiol. 122, 1119–1127.

Sasaki, S., Nishida, T., Tsutsumi, Y., Kondo, R., 2004. Lignin dehydrogenative polymerization mechanism: a poplar cell wall peroxidase directly oxidizes polymer lignin and produces *in vitro* dehydrogenative polymer rich in beta-*O*-4 linkage. FEBS Lett. 562, 197–201.

Syrjanen, K., Brunow, G., 2000. Regioselectivity in lignin biosynthesis. The influence of dimerization and cross-coupling. J. Chem. Soc. Perkin Trans. 1, 183–187.

Takahama, U., Oniki, T., 1994. Effects of ascorbate on the oxidation of derivatives of hydroxycinnamic acid and the mechanism of oxidation of sinapic acid by cell wall-bound peroxidases. Plant Cell Physiol 35, 593–600.

Takahama, U., Oniki, T., Shimokawa, H., 1996. A possible mechanism for the oxidation of sinapyl alcohol by peroxidase-dependent reactions in the apoplast: enhancement of the oxidation by hydroxycinnamic acids and components of the apoplast. Plant Cell Physiol. 37, 499–504.

Tobimatsu, Y., Takano, T., Kamitakahara, H., Nakatsubo, F., 2008a. Studies on the dehydrogenative polymerizations (DHPs) of monolignol beta-glycosides: Part 4. Horseradish peroxidase-catalyzed copolymerization of isoconiferin and isosyringin. Holzforschung 62, 495–500.

Tobimatsu, Y., Takano, T., Kamitakahara, H., Nakatsubo, F., 2008b. Studies on the dehydrogenative polymerization of monolignol beta-glycosides: Part 5. UV spectroscopic monitoring of horseradish peroxidase-catalyzed polymerization of monolignol glycosides. Holzforschung 62, 501–507.

Tobimatsu, Y., Takano, T., Kamitakahara, H., Nakatsubo, F., 2008c. Studies on the dehydrogenative polymerizations of monolignol beta-glycosides. Part 3: Horseradish peroxidase-catalyzed polymerizations of triandrin and isosyringin. J. Wood Chem. Technol. 28, 69–83.

Tobimatsu, Y., Takano, T., Kamitakahara, H., Nakatsubo, F., 2010. Studies on the dehydrogenative polymerization of monolignol beta-glycosides. Part 6: Monitoring of horseradish peroxidase-catalyzed polymerization of monolignol glycosides by GPC–PDA. Holzforschung 64, 173–181.